

Scaling electrical percolation networks based on renormalization group theory

Weijian Li^{1,2†}, Yan He^{2†}, Kaiyuan Yang² and Gururaj Naik^{2*}

¹Applied Physics Program, Rice University, 6100 Main St., Houston, 77005, TX, USA.

²Electrical & Computer Engineering, Rice University, 6100 Main St., Houston, 77005, TX, USA.

*Corresponding author(s). E-mail(s): guru@rice.edu;
Contributing authors: weijian.li@rice.edu; yan.he@rice.edu;
kaiyuan.yang@rice.edu;

†These authors contributed equally to this work.

Abstract

Many natural disordered systems such as percolation metal films may be approximated as fractals. Probing their properties can be difficult depending on the length scale involved. Often, characterizing the system at a convenient length scale and building models for extrapolating the measured data to other length scales is preferred. In such situations, a general algorithm for scaling the model network while preserving its statistical equivalence is required. Here, we provide an algorithm that draws inspiration from renormalization group theory for scaling disordered fractal networks. This algorithm includes three steps: expand, map, and reduce resolution, where the mapping is the only computationally expensive step. We describe a way to minimize the computational burden and accurately scale the model network. We experimentally validate the algorithm in a percolating electrical network formed by an ultra-thin gold film on a glass substrate. By measuring the resistance between many pairs of pads separated by a given length, we accurately predict the mean and standard deviation of the resistance distribution measured across pads separated by twice the original distance. The algorithm presented here is general and may be applied to any disordered fractal system.

Keywords: Disordered system, Electrical conduction, Ultra-thin metal films, Percolation networks

1 Introduction

Percolation theory is a simple and powerful statistical model to study phase transitions and other interesting phenomena in disordered systems around their critical points [1–8]. This mathematical model appropriately describes the statistical behavior of many networks and has been applied to a wide range of fields in nature from biology and sociology, to statistical physics and computer science [7, 9–17]. Geometrical scaling is an important application of such model [18]. A physical property of the network measured at some convenient length scale could be extrapolated to the same measured at any other length scale as required by the application. For example, consider an application where the electrical resistance distribution in a percolation metal network is required at a pad separation of 1 mm. Suppose the experimental setup limits the pad separation to 100 μm at the most. In this case, geometrical scaling could be applied to the experimental data measured at 100 μm pad separation to generate an equivalent resistance distribution at a pad separation of 1 mm. Such geometrical scaling methods exist for some special percolation lattices such as 2D Bethe lattices [19, 20]. However, a general scaling method applicable for any percolation network remains to be developed. Here, we propose and experimentally validate such a scaling algorithm for a 2D percolation network. Our approach is inspired by the renormalization group theory.

Renormalization group (RG) theory is a framework typically used to study the topology of quantum many-body systems at different scales [21–29]. RG theory based on the self-similarity of the systems near the critical points deals with the divergence of complex networks at their phase transitions. Inspired by the RG theory and the similarity of the percolation threshold to critical points of a quantum many-body system, we demonstrate an algorithm to scale percolation networks.

Our algorithm considers a 2D percolation network. Fig. 1(a) shows a typical 2D-site percolating network with two different types of occupations. Since the elements are randomly distributed, the properties of the network depend on the fill factor p of one of the elements. Assuming that the network is a grid of $n \times n$ sites with each site occupying $a \times a$ area, let θ_{n*a} be the central tendency of some property of this network measured at a length scale d proportional to a . An example of such a property is the resistance of a 2D electrical percolation network measured across a given distance d . θ_{n*a} is dependent on the fill fraction p of the 2D percolation network and the length scale a . Suppose, we scale or zoom out by a factor s ($s > 1$) and measure the same property of the network at a scaled length scale $d \propto s \times a$, the corresponding central tendency θ_{n*sa} will be different and depends on s , a , and p as indicated in Fig. 1(b). In the example of an electrical percolation network, it could be harder to measure resistances on a larger network at a larger length scale $s \cdot a$ than at a . In such cases, can we measure the original network and sufficiently model the zoomed-out network? More conveniently, can we find some other fill factor p' for the scaled original network to model the zoomed-out network? Mathematically, can we find p' such that $\theta_{sn*a}(p) = \theta_{n*sa}(p')$? The goal of this work is to find

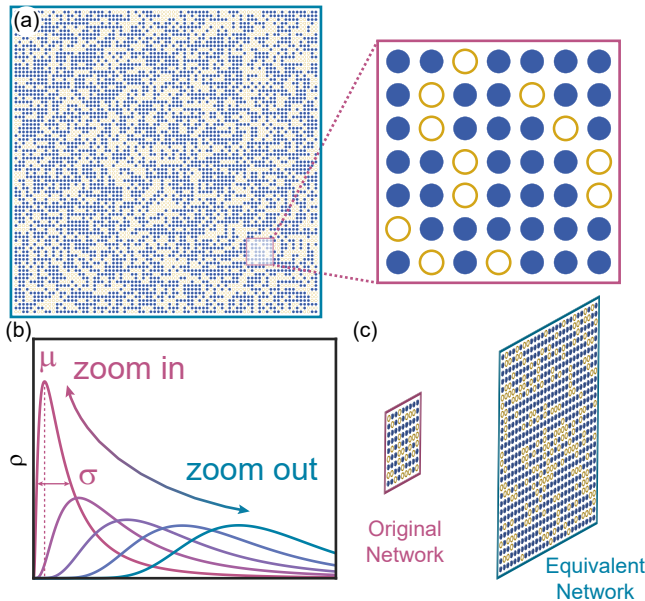


Fig. 1 Renormalization for 2D percolation networks: (a) A schematic of a 2D-site percolation system with the filling factor p at zoom-out (left, green) and zoom-in (right, red) scales. The blue dots and yellow circles denote two different filling elements. (b) The central tendency of a property θ varies at different scales. Here we use log-normal distributions as examples. σ and μ are the log-mean value and standard deviation of the log-normal distribution. ρ is the probability function. (c) The generated large network has same number of discrete elements as the original, has a different fill factor p' , and is statistically equivalent to the original network.

an equivalent network at the zoomed-out length scale $\times a$ using the original network (Fig. 1(c)). We present an algorithm to construct such equivalent networks and validate them by measuring electrical resistances in a percolating network of conductors formed by ultra-thin gold films on glass substrates.

2 Scaling algorithm

The central idea of our algorithm is illustrated in Fig. 2. Consider a finite-sized original network consisting of $n \times n$ sites with the size of each site $a \times a$. Two types of elements randomly occupy the network with a fill fraction p for one of the elements. The statistical parameter set of this percolation network is represented as $\theta_{n \cdot a}(p)$ as shown in Fig. 2(a). In a single iteration, we first multiply the number of sites in each dimension by a scaling factor s to generate a new expanded network. Figure 2(b) shows this procedure for $s = 2$. The new network consists of $sn \times sn$ sites. The size of each site is still the same as the original ($a \times a$) and the total length scale of the network becomes s times larger ($s \cdot a$). Then, the statistical parameter set of the expanded network is represented as $\theta_{sn \cdot a}(p)$. Since the two networks share the same fill factor p but are different in the length scale, the statistics exhibit different behavior,

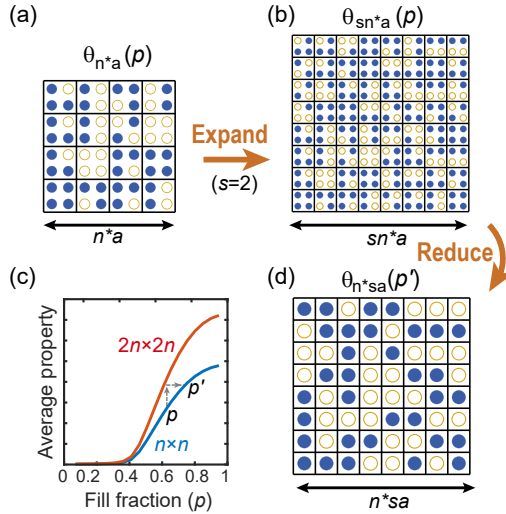


Fig. 2 The scaling algorithm for a 2D-site percolation network: (a) The original network consisting $n \times n$ ($n = 8$ here) sites of size $a \times a$ with a fill fraction p for one of the elements. The desired statistical parameter of the network is represented as $\theta_{n \cdot a}(p)$. (b) First step is to expand the network by scaling the number of sites in both the dimensions from n to $s \cdot n$ ($s=2$ here). The size of each site is still $a \times a$ in the expanded network. The desired parameter of the new network is represented as $\theta_{s \cdot n \cdot a}(p)$. (c) The average of the desired property of the network calculated from Monte Carlo simulations for the original and the expanded networks. Dotted lines show how to find the new fill factor p' for the equivalent network. (d) The equivalent network generated by reducing the resolution of the expanded network. The equivalent network has $n \times n$ sites of $sa \times sa$ area. The statistical parameter of the equivalent network is the same as the enlarged network, $\theta_{n \cdot sa}(p') = \theta_{s \cdot n \cdot a}(p)$.

$\theta_{n \cdot a}(p) \neq \theta_{s \cdot n \cdot a}(p)$. To generate an equivalent network, we renormalize the expanded percolation network by reducing it back to $n \times n$. We carry out this reduction in such a way that the average of the desired property of the network is kept unchanged. This transformation is carried out with the help of Monte Carlo simulations and is the only computationally expensive step. We generate two curves corresponding to the mean value of the desired property $\mu(p)$ on $n \times n$ and $s \cdot n \times s \cdot n$ networks as shown in Fig. 2(c). We use these curves to find a p' for the reduced network that keeps the average property unchanged. The procedure for finding this p' is shown by the dotted lines in Fig. 2(c). In the first step of the algorithm, we expanded the network from $n \times n$ to $s \cdot n \times s \cdot n$ at constant p which is represented by the vertical arrow from the $n \times n$ curve to $s \cdot n \times s \cdot n$ curve. Then, the reduction step is represented by a horizontal move where the average property is held constant. After the reducing step, we generate an equivalent $n \times n$ network with a different fill factor p' . This new network is the equivalent of the scaled original one: $\theta_{n \cdot sa}(p') = \theta_{s \cdot n \cdot a}(p)$.

The reduction is the key step in the algorithm that differs from the traditional RG theory used in solid-state physics. For example, in renormalization applied to the Ising model, the renormalized spin occupancy in the new lattice

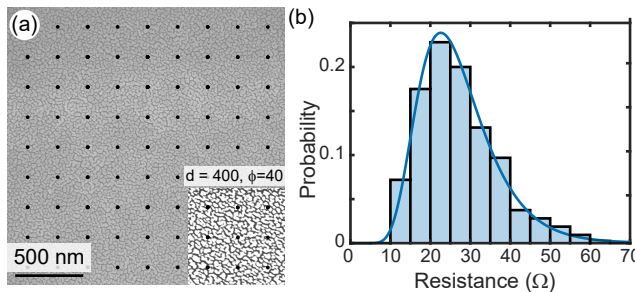


Fig. 3 Electric resistance simulation of an ultra-thin metallic film on insulating substrate: (a) SEM image of 7.5 nm gold on SiO_2 substrate. The inset is the binarized image. The dark dots denote the contact pads. The diameter of pads is $\phi=40$ pixels and separated by $d=400$ pixels. (b) The normalized resistance distribution of the digitized device in (a). The solid line is the fitted log-normal distribution function.

is determined by the majority spin in the corresponding original lattice [30–32]. Such a renormalization relationship is not unique and leads the system to shift toward phase divergence. Comparatively, our algorithm constrains the network to keep the same statistical properties at each renormalization step and solve the renormalization relationship accordingly. As a result, the phase of the system fixes at a certain point. In other words, our algorithm maintains all the statistical properties of the network.

Our reduction step also implements the necessary generalization of geometrical scaling of percolation Bethe lattices. The two curves of Fig. 2(c) are generated from simulations rather than from analytical models. Analytical models are easy on special lattices such as 2D Bethe lattice. However, for a general percolation lattice, simulations allow generalization. Simulations may be carried out using any available technique. Monte Carlo method is used here only because of its relative ease of implementation. However, powerful deep learning techniques could be beneficial for more complex problems such as 3D networks [33–35].

Since reduction is the only computationally intensive step here, using the smallest possible value of s , i.e., $s = 2$, is computationally advantageous. If the desired final scaling factor $s = 2^m$, then m iterations of this scaling algorithm lead to the equivalent network. Note that the Monte Carlo simulations in this iterative application of the algorithm need to be carried out only once to generate the curves for $n \times n$ and $2n \times 2n$ networks. Also, it is clear from Fig. 2(c) that equivalent networks are not guaranteed to exist for all values of s . However, when they exist, our algorithm precisely generates them.

3 Experimental results and discussions

We validate our RG theory-based scaling algorithm in ultra-thin metal films. Ultra-thin metallic films are known to behave as 2D electrical percolation systems [36–38]. We study the electrical resistance of ultra-thin gold film on an insulating substrate. Our system comprises of electron beam evaporated 7.5

6 *Renormalizing percolation networks*

nm thick gold on a silicon oxide substrate. The thickness numbers here are as measured by a quartz crystal monitor. Fig. 3(a) shows the SEM image of the sample. The microstructure of this sample consisting of a random distribution of gold islands confirms the 2D electrical percolation network. We convert the grayscale SEM images to black-and-white images using a binarization procedure. The binarized 1600×1600 pixel matrices are used in all further analyses. First, we add an array of contact pads to mimic real resistance measurements, as shown in the inset of Fig. 3(a). Then, we numerically measure the resistance of the films and generate the statistics using HSPICE, a commercial simulator. We assume that the electrical resistance of each white pixel (gold) is 1Ω and the resistance of each dark pixel is 500Ω . The resistance of the dark pixel can be any large quantity, but too large a number makes the resistance distribution bimodal. The contact pads are 40 pixels in diameter denoted by $\phi = 40$ and separated by $d=400$ pixels. We calculated the resistance between 500 pairs of adjacent pads and found the statistical distribution shown in Fig. 3(b). The distribution can be perfectly fitted by a log-normal function as expected for a percolation network.

Next, we apply the renormalization algorithm to the resistance distribution in this 2D percolation system. We first binarize our percolation sample's SEM image of area $650 \times 650 \text{ nm}^2$ shown in Fig. 4(a). After binarization, we generate 130×130 square pixel matrix shown in Fig. 4(b) with $p=0.27$. The pad diameter ϕ and the distance between pads d are indicated on the figure panels. The resistance distributions for the original sample and the binarized network are shown in Fig. 4(c). Next, we expand the original network by two in each dimension to obtain the center network of Fig. 4(b). Compared to the original network, we found that the log-mean value of the resistance distribution in this larger network shifts from 3.24 to 3.65, a trend expected from Fig. 2(c).

Then, we make use of Fig. 2(c) to find p' for reducing this expanded network. For Fig. 2(c), we run Monte Carlo simulations to generate a series of 2D electrical percolation networks with different fill fractions p and calculate the mean resistance across as a function of p . We carry out these simulations for a pad separation of 100 pixels on two networks of sizes: 130×130 and 260×260 . From the curves of Fig. 2(c), we find $p'=0.285$ for the equivalent network.

Next, we generate a reduced resolution network, 130×130 where each pixel now corresponds to twice the physical length of the pixels in the original network. The reduced network shown in the right panel in Fig. 4(b) corresponds to the fill fraction $p'=0.285$. The mean and standard deviations of this model network are compared against those computed on the actual sample in the right panel of Fig. 4(c). Both the actual sample and the model at double length scale possess log-normal resistance distributions. The mean value of the resistance in both actual and model networks agrees well. However, the standard deviations differ here only because the binarized network generated from the original (left panel of Fig. 4(a)) deviates in its standard deviation. But, the relative changes in the standard deviations are consistent across the binarized networks and their corresponding SEM images. For example, the standard

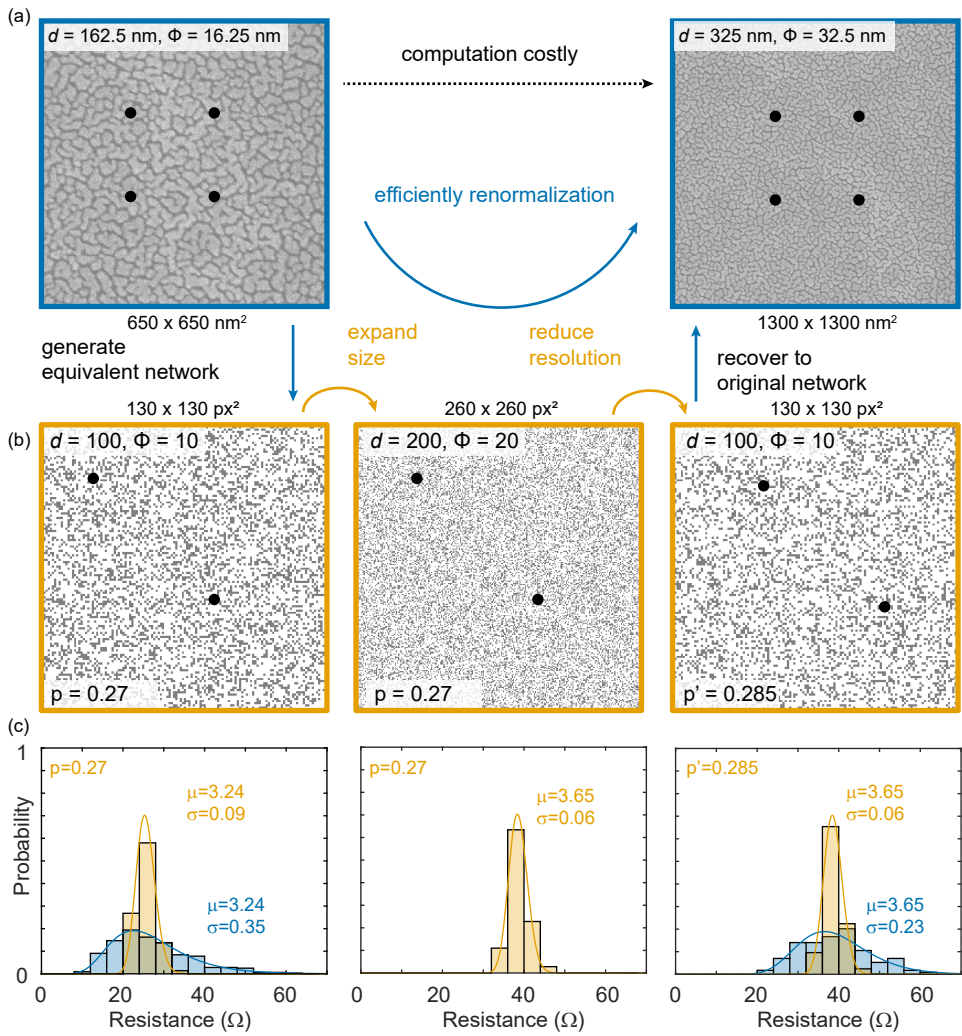


Fig. 4 Renormalization algorithm applied to a 2D electrical percolation network formed by ultra-thin film of gold on glass: (a) The SEM image of the original (left) and the zoomed out (right) regions of the samples considered for the analysis. The physical dimensions of the SEM images are mentioned at their bottom. The four black dots represent an array of contact pads for electrical resistance measurements. The distance d between contact pads and the pad diameter ϕ are indicated inside the panels. (b) The binarized representative networks corresponding to the real samples in (a). The area of the model networks are represented above them in squared pixels (px). d and ϕ are in pixel units. The three model networks correspond to the outcomes of three steps in our renormalization algorithm. (c) The calculated normalized electrical resistance distributions for the real (blue) and the model (yellow) networks shown in rows above. The solid curves are the fitted log-normal function. The log-mean μ and standard deviation σ values are indicated for both curves in ohm.

deviation of the binarized original network is 0.09 and it scales down to 0.06 for the model network at the double-length. This corresponds to a scaling factor of 0.67. Applying the same scaling factor to the standard deviation of the original SEM image leads to $\sigma=0.35\times0.67=0.23$. This standard deviation result agrees well with the computed value for the SEM image on the right panel of Fig. 4(a). Thus, the model network our algorithm accurately predicts the resistance distribution at the double-length scale.

4 Conclusion

In conclusion, we outlined an algorithm based on renormalization group theory to build model networks of a percolation network at any zoom factor or length scale. The three-step algorithm involved modeling the original network at the original length scale, expanding the physical size of the model at the same length resolution, and reducing the resolution to that of the original network while preserving the average properties. The computationally most expensive step was the last one where Monte Carlo simulations were employed. Also, the key difference between our algorithm and the traditional renormalization group theory is in the last step where we preserve the average properties of the network to avoid phase divergences. We demonstrated the operation of our algorithm in an electrical percolation system made of ultra-thin gold films on an insulating substrate. The resistance distribution predicted by our algorithm for a zoom factor of two agreed well with that of the actual sample measured at a double-length scale. Generalizing the result, our algorithm works for any zoom factor as long as there exists an equivalent network at that zoom factor. Our algorithm may be applied not only to percolation systems but also to any other stochastic fractal network. It provides a convenient way to build simple models of complex disordered networks.

Declarations

- Funding This work was supported by the National Science Foundation grant ECCS-2028997.
- Availability of data and materials The datasets generated during and/or analysed during the current study are available from the corresponding author on reasonable request.

References

- [1] Shante, V.K., Kirkpatrick, S.: An introduction to percolation theory. *Advances in Physics* **20**(85), 325–357 (1971)
- [2] Kirkpatrick, S.: Percolation and conduction. *Reviews of modern physics* **45**(4), 574 (1973)

- [3] Essam, J.W.: Percolation theory. *Reports on progress in physics* **43**(7), 833 (1980)
- [4] Stauffer, D., Aharony, A.: *Introduction to Percolation Theory*. Taylor & Francis, London (2018)
- [5] Bollobás, B., Bollobás, B., Riordan, O.: *Percolation*. Cambridge University Press, New York (2006)
- [6] Meester, R., Roy, R.: *Continuum Percolation* vol. 119. Cambridge University Press, New York (1996)
- [7] Sahimi, M.: *Applications of Percolation Theory*. CRC Press, London (1994)
- [8] Xu, W., Jiao, Y.: Theoretical framework for percolation threshold, tortuosity and transport properties of porous materials containing 3d non-spherical pores. *International Journal of Engineering Science* **134**, 31–46 (2019)
- [9] Berkowitz, B., Balberg, I.: Percolation theory and its application to groundwater hydrology. *Water Resources Research* **29**(4), 775–794 (1993)
- [10] Saberi, A.A.: Recent advances in percolation theory and its applications. *Physics Reports* **578**, 1–32 (2015)
- [11] Gao, J., Buldyrev, S.V., Stanley, H.E., Xu, X., Havlin, S.: Percolation of a general network of networks. *Physical Review E* **88**(6), 062816 (2013)
- [12] Riordan, O., Warnke, L.: Explosive percolation is continuous. *Science* **333**(6040), 322–324 (2011)
- [13] Araújo, N., Grassberger, P., Kahng, B., Schrenk, K., Ziff, R.M.: Recent advances and open challenges in percolation. *The European Physical Journal Special Topics* **223**(11), 2307–2321 (2014)
- [14] da Costa, R.A., Dorogovtsev, S.N., Goltsev, A.V., Mendes, J.F.F.: Explosive percolation transition is actually continuous. *Physical review letters* **105**(25), 255701 (2010)
- [15] Radicchi, F.: Percolation in real interdependent networks. *Nature Physics* **11**(7), 597–602 (2015)
- [16] Marsden, A.J., Papageorgiou, D., Valles, C., Liscio, A., Palermo, V., Bissett, M., Young, R., Kinloch, I.: Electrical percolation in graphene–polymer composites. *2D Materials* **5**(3), 032003 (2018)
- [17] Xu, W., Zhang, Y., Jiang, J., Liu, Z., Jiao, Y.: Thermal conductivity and

10 *Renormalizing percolation networks*

elastic modulus of 3d porous/fractured media considering percolation. International Journal of Engineering Science **161**, 103456 (2021)

- [18] Xu, W., Zhu, Z., Jiang, Y., Jiao, Y.: Continuum percolation of congruent overlapping polyhedral particles: Finite-size-scaling analysis and renormalization-group method. Physical Review E **99**(3), 032107 (2019)
- [19] De Pádua, A., De Miranda-Neto, J.A., Moraes, F.: Geometrical scaling in the bethe lattice. Modern Physics Letters B **08**(14n15), 909–915 (1994). <https://doi.org/10.1142/S0217984994000911>
- [20] Molnar, P.: On geometrical scaling of cayley trees and river networks. Journal of hydrology **322**(1-4), 199–210 (2006)
- [21] Young, A., Stinchcombe, R.: A renormalization group theory for percolation problems. Journal of Physics C: Solid State Physics **8**(23), 535 (1975)
- [22] Harris, A.B., Lubensky, T.C., Holcomb, W.K., Dasgupta, C.: Renormalization-group approach to percolation problems. Physical Review Letters **35**(6), 327 (1975)
- [23] Reynolds, P.J., Stanley, H., Klein, W.: A real-space renormalization group for site and bond percolation. Journal of Physics C: Solid State Physics **10**(8), 167 (1977)
- [24] Stauffer, D.: Scaling theory of percolation clusters. Physics reports **54**(1), 1–74 (1979)
- [25] Reynolds, P.J., Stanley, H.E., Klein, W.: Large-cell monte carlo renormalization group for percolation. Physical Review B **21**(3), 1223 (1980)
- [26] Sahimi, M., Hughes, B.D., Scriven, L., Davis, H.T.: Real-space renormalization and effective-medium approximation to the percolation conduction problem. Physical Review B **28**(1), 307 (1983)
- [27] Derrida, B., Seze, L.D.: Application of the phenomenological renormalization to percolation and lattice animals in dimension 2. In: CARDY, J.L. (ed.) Finite-Size Scaling. Current Physics–Sources and Comments, vol. 2, pp. 275–283. Elsevier, ??? (1988). <https://doi.org/10.1016/B978-0-444-87109-1.50024-8>
- [28] Kieling, K., Rudolph, T., Eisert, J.: Percolation, renormalization, and quantum computing with nondeterministic gates. Physical Review Letters **99**(13), 130501 (2007)
- [29] Karschau, J., Zimmerling, M., Friedrich, B.M.: Renormalization group

theory for percolation in time-varying networks. *Scientific reports* **8**(1), 1–8 (2018)

- [30] Pawley, G., Swendsen, R., Wallace, D., Wilson, K.: Monte carlo renormalization-group calculations of critical behavior in the simple-cubic ising model. *Physical Review B* **29**(7), 4030 (1984)
- [31] Baillie, C.F., Gupta, R., Hawick, K.A., Pawley, G.S.: Monte carlo renormalization-group study of the three-dimensional ising model. *Physical Review B* **45**(18), 10438 (1992)
- [32] Binder, K., Luijten, E.: Monte carlo tests of renormalization-group predictions for critical phenomena in ising models. *Physics Reports* **344**(4-6), 179–253 (2001)
- [33] Zhang, W., Liu, J., Wei, T.-C.: Machine learning of phase transitions in the percolation and x y models. *Physical Review E* **99**(3), 032142 (2019)
- [34] Shen, J., Li, W., Deng, S., Zhang, T.: Supervised and unsupervised learning of directed percolation. *Physical Review E* **103**(5), 052140 (2021)
- [35] Fu, J., Xiao, D., Li, D., Thomas, H.R., Li, C.: Stochastic reconstruction of 3d microstructures from 2d cross-sectional images using machine learning-based characterization. *Computer Methods in Applied Mechanics and Engineering* **390**, 114532 (2022)
- [36] Neugebauer, C., Webb, M.: Electrical conduction mechanism in ultrathin, evaporated metal films. *Journal of Applied Physics* **33**(1), 74–82 (1962)
- [37] Kazmerski, L., Racine, D.M.: Growth, environmental, and electrical properties of ultrathin metal films. *Journal of Applied Physics* **46**(2), 791–795 (1975)
- [38] Hövel, M., Gompf, B., Dressel, M.: Dielectric properties of ultrathin metal films around the percolation threshold. *Physical Review B* **81**(3), 035402 (2010)